ELSEVIER

European Polymer Journal 37 (2001) 2295–2312

EUROPEAN POLYMER JOURNAL

www.elsevier.com/locate/europolj

Vibrational dynamics and phonon dispersion in poly(β-benzyl-L-aspartate) (β-sheet)

K.J. Maria Das [1], Shantanu Rastogi [2], Poonam Tandon, V.D. Gupta *

Department of Physics, Lucknow University, Lucknow 226 007, India

Received 23 June 2000; received in revised form 8 January 2001; accepted 20 March 2001

Abstract

Poly(β-benzyl-L-aspartate) (PBLA) shows unusual conformational variety and under varying conditions of preparation it is capable of adopting four different conformations, namely left-handed α helix (α_l), right-handed α helix (α_r), ω helix and β pleated sheet. We present here a complete phonon dispersion and heat capacity study on the β form of PBLA. A comparison of the characteristic features and the conformational dependence of modes for α, β and ω forms of PBLA are made. It is observed that the dispersion of modes in the β form is in general larger than in the α form. Crossing over and repulsion of various dispersion branches are discussed.

Keywords: Phonons; Dispersion; Crossing over; Repulsion; Heat capacity

1. Introduction

Poly(β-benzyl-L-aspartate) (PBLA) is a synthetic homopolypeptide, which shows unusual conformational variety. Under varying conditions of preparation it is capable of adopting four different conformations, namely left-handed α helix (α_l), right-handed α helix (α_r), ω helix and β pleated sheet [1–6]. This conformational versatility of PBLA has made it an interesting model for the study of molecular dynamics of proteins and polypeptides. PBLA forms a left-handed α helix when films are cast from solvent, the vibrational dynamics for this form has been reported earlier [7]. The unusual left-handed helix sense for α and ω forms could be related to lesser steric hindrance produced at β carbon as compared to the right-handed form [5]. Films of low-molecular weight PBLA are converted to the cross β sheet conformation when heated at 140°C, while films of higher molecular weight form the ω helix after identical heat treatment. On further heating the ω form turns irreversibly into β pleated sheet conformation [8–10]. The irreversibility is due to the formation of interchain hydrogen bonds. In this communication we report complete phonon dispersion and heat capacity for the β form of PBLA.

Earlier studies on the dispersion curves of polyglycine I, poly(L-alanine), poly(L-serine) and poly(L-valine) [11–14] in β sheet conformation show that the amide as well as other skeletal modes and their dispersive behaviour depend not only on the backbone conformation but also on the side-chain structure. Dispersion curves for the α and ω forms of PBLA have been recently reported by Tandon et al. [7] and Gupta [15]. However no such studies have been reported on the β form. In the present work we report a comparison of the characteristic features of the dispersion curves for α, β and ω forms of PBLA.

Frushour and Koenig [16] have reported infrared (IR) and Raman spectroscopic studies for β-PBLA. Their assignments are based on qualitative considerations and are incomplete specially in the low-frequency region. Hence, a complete normal mode analysis and their dispersion for β-PBLA has been carried out. Further, under certain conditions the regions of high density of-states

* Corresponding author. Fax: +91-522-223-405/938.

E-mail addresses: vdgl@rediffmail.com, root@cscdri.ren.nic.in (V.D. Gupta).

[1] Department of Radiotherapy, Sanjay Gandhi Post Graduate Institute of Medical Science, Lucknow 226 014, India.

[2] Presently at Department of Physics, DDU Gorakhpur University, Gorakhpur 273 009, India.

0014-3057/01/$ - see front matter
PII: S0014-3057(01)00096-9

and profile of the dispersion curves may be reflected in the absorption spectra. In addition, correlation between macroscopic properties and microscopic behaviour can be obtained from the heat capacity evaluation. The normal modes for N-deuterated system have also been calculated to check the validity of assignments and force field. Predictive values of heat capacity are reported and a comparison with α and ω forms is made.

2. Theory and experiment

2.1. Calculation of normal mode frequencies

The calculation of normal mode frequencies has been carried out according to Wilson's G.F. matrix method [17] as modified by Higgs [18] for an infinite chain. In brief, the vibrational secular which gives normal mode frequencies and their dispersion as a function of phase angles has the form:

$$[G(\delta)F(\delta) - \lambda(\delta)I] = 0, \quad 0 < \delta < \pi \tag{1}$$

where G is the inverse of the kinetic energy matrix, F is the force field matrix, δ is the vibrational phase difference between the corresponding modes of the adjacent residue units.

The vibrational frequencies $v(\delta)$ (in cm^{-1}) are related to eigenvalues $\lambda(\delta)$ by the following relation:

$$\lambda(\delta) = 4\pi^2 c^2 v^2(\delta) \tag{2}$$

The calculated frequencies at $\delta = 0$ and $\delta = \pi$ are matched with the observed IR and Raman frequencies reported by Frushour and Koenig [16].

2.2. Calculation of specific heat

Dispersion curves can be used to calculate the specific heat of a polymeric system. For a one-dimensional system the density-of-state function or the frequency distribution function, which expresses the way energy is distributed among the various branches of normal modes in the crystal, is calculated from the relation:

$$g(v) = \sum_j (\partial v_j/\partial\delta)^{-1}\Big|_{v_j(\delta)=v} \quad \text{with} \quad \int g(v_j)\partial v_j = 1 \tag{3}$$

The sum is over branches j. Considering a solid as an assembly of harmonic oscillators, the frequency distribution $g(v)$ is equivalent to a partition function.

The specific heat capacity, if interpreted right, can give information about the proportion of various conformational states present in the material. For example, in case of a protein it can give information about the proportion, which is in α helical or β sheet structure. This is necessary in evaluating the basic thermodynamics of enzyme reaction [19]. The constant volume heat capacity can be calculated using Debye's relation

$$C_v = \sum_j g(v_j) k N_A (h v_j/kT)^2 \frac{\exp(h v_j/kT)}{[\exp(h v_j/kT) - 1]^2} \tag{4}$$

where k is the Boltzmann constant, N_A is the Avogadro number, h is Planck's constant, v_j is the frequency of the jth mode and T is the absolute temperature.

The constant volume heat capacity C_v, given by Eq. (3) can be converted into constant pressure heat capacity C_p using the Nernst–Lindemann approximation [20]

$$C_p - C_v = 3RA_0(C_p^2 T/C_v T_m) \tag{5}$$

where A_0 is a constant often of a universal value (3.9×10^{-9} (K mol)/J), T_m is the estimated equilibrium melting temperature and R is the gas constant [21]. Since experimental data on specific heat of PBLA has not been reported, only the predictive values of C_v have been obtained.

3. Results and discussion

In β-PBLA, there are 26 atoms per residue unit (Fig. 1), giving rise to 78 dispersion curves. The vibrational

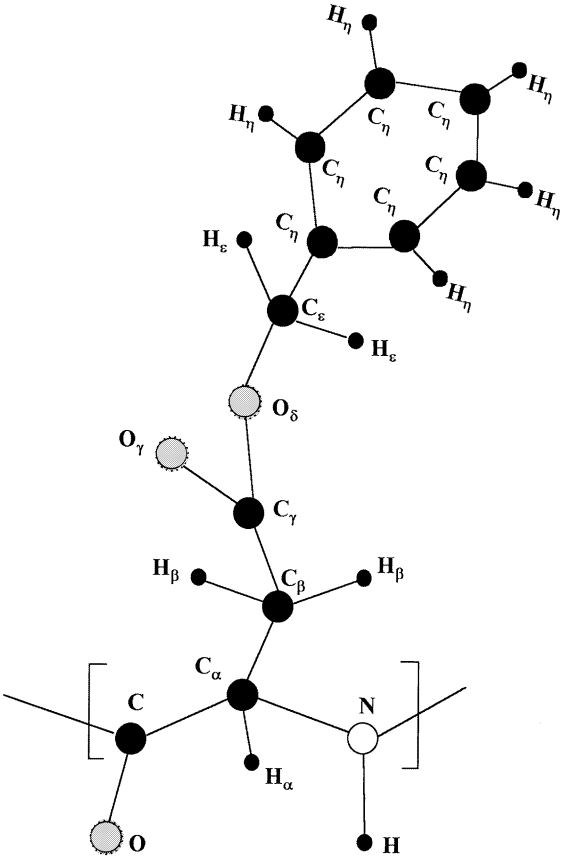

Fig. 1. One chemical repeat unit of PBLA.

frequencies have been calculated for δ values ranging from 0 to π in steps of 0.05π. The optically active modes are those for which $\delta = 0$ or π. All the modes above 1400 cm^{-1} except amide I and II are nondispersive, hence only modes below this are shown in Figs. 2(a)–5(a). Initially the force constants for the backbone of β-PBLA have been taken from the β poly(L-alanine) [12] and for the side chain are transferred from α_l-PBLA [7]. These are then modified to give the "best fit" to the reported spectroscopic data from IR and Raman [16]. The assignments of normal mode frequencies are based on the potential energy distribution (PED), line strength, line shape and the presence/absence of similar groups in identical environments. The assignments made by us using the above criteria are in agreement with the ones reported by Frushour and Koenig [16] in the neighbourhood of zone centre. These authors have not reported the ring modes, nor have they reported dispersions of the normal modes. We have filled in all these gaps. The final set of force constants are given in Table 1.

The two lowest lying branches in the dispersion curves ($v = 0$ at $\delta = 0$ and $\delta = \pi$) are the four acoustic modes which correspond to the rotation about helix axis and translations parallel and perpendicular to the helix axis.

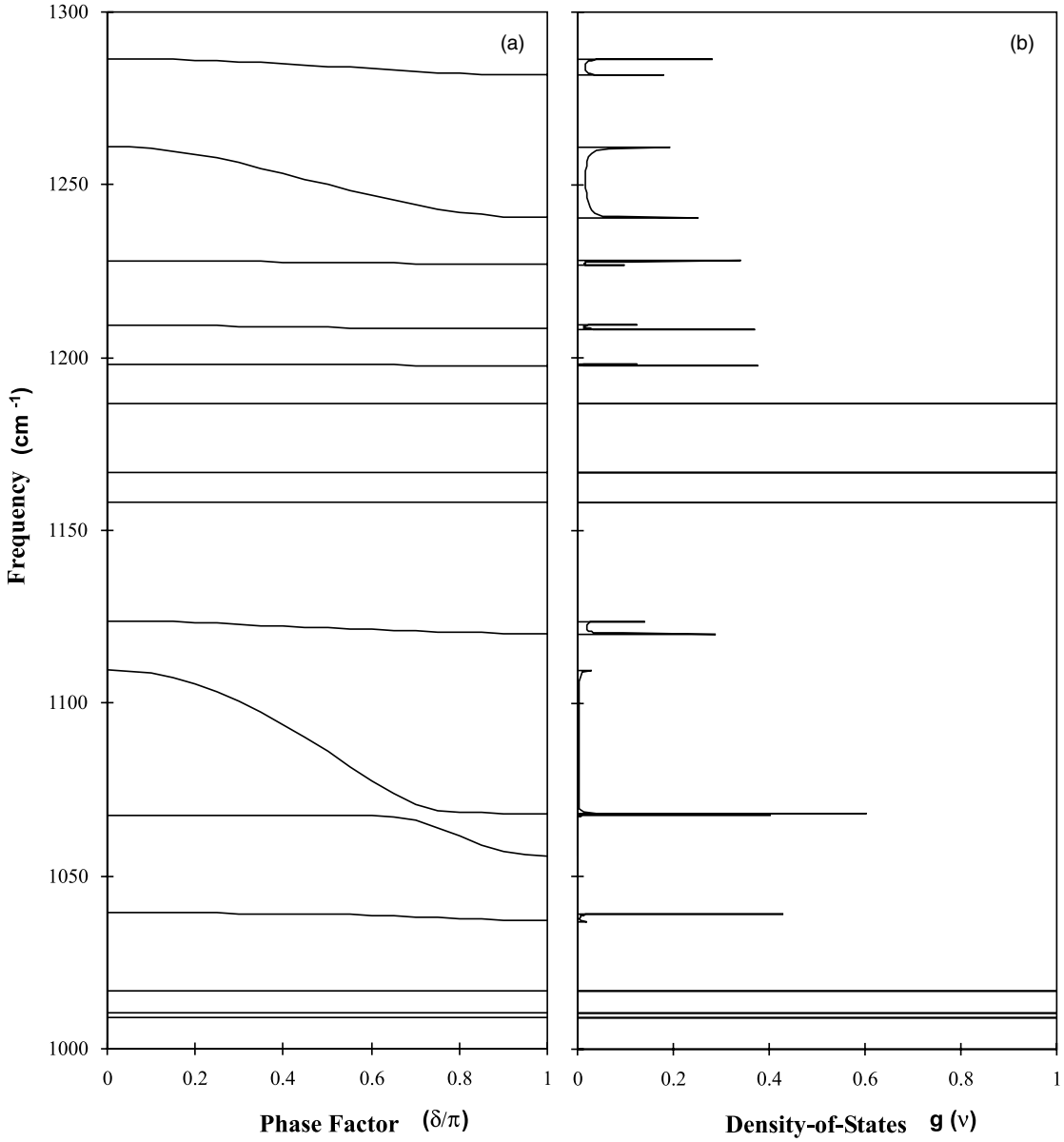

Fig. 2. (a) Dispersion curves (1300–1000 cm^{-1}). (b) Density of states (1300–1000 cm^{-1}).

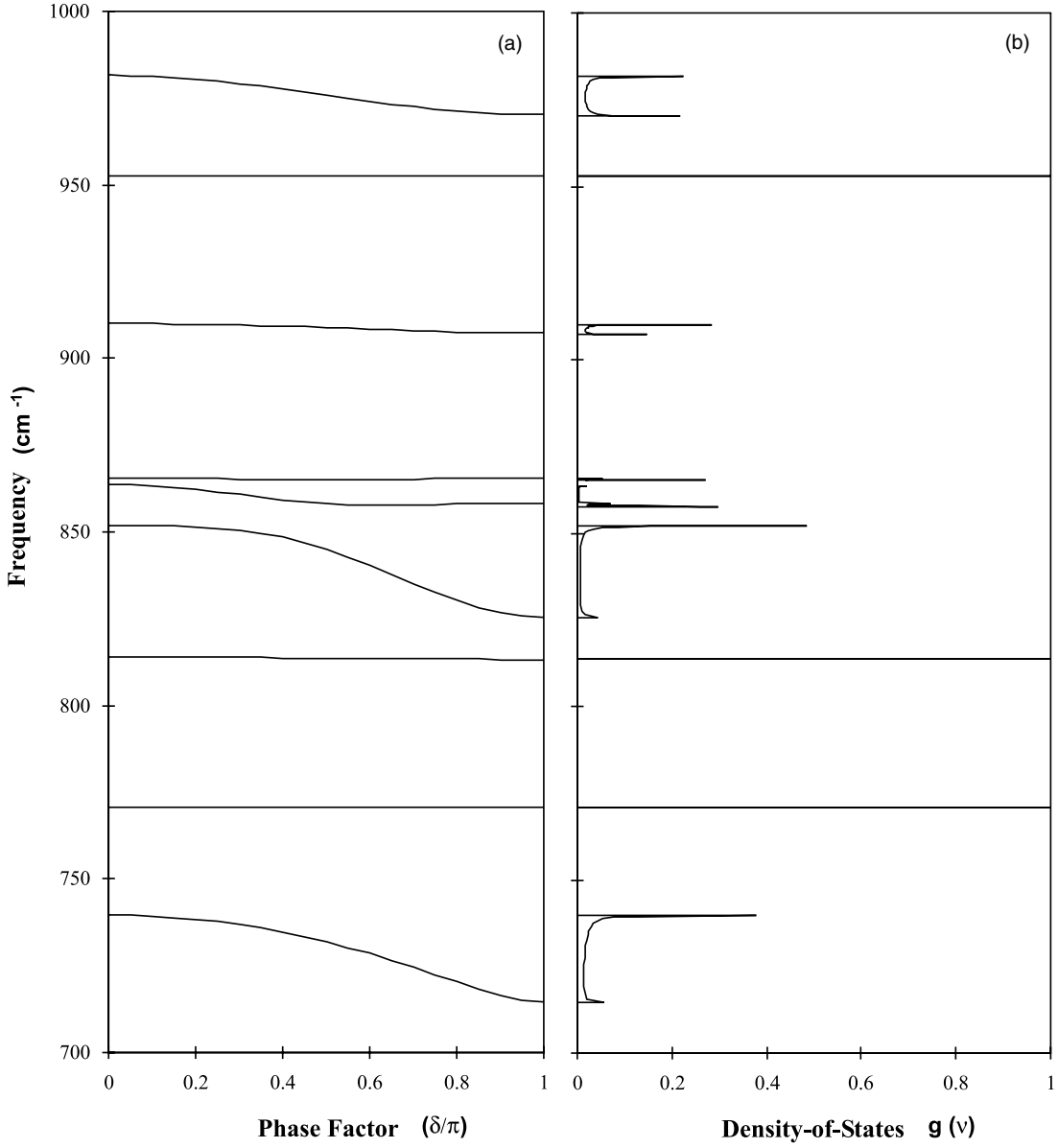

Fig. 3. (a) Dispersion curves (1000–700 cm^{-1}). (b) Density of states (1000–700 cm^{-1}).

For the sake of simplicity the modes are discussed under two separate sections viz. backbone and side-chain modes. Mixed modes are the ones, which have PED arising from both of these. They show maximum dispersion and therefore are discussed in the section on dispersion curves.

3.1. Backbone modes

Generally the modes involving the motion of amide group, [–NH–C═O–], are regarded as backbone modes. The normal mode analysis shows that unlike the low-frequency region there is very little coupling between skeletal and side-chain modes in the 3350–1400 cm^{-1} region. The pure backbone at $\delta = 0$ and π modes are shown in Table 2. The modes which involve the motion of the ring, other side-chain atoms and the mixed modes are given in Tables 6–8 respectively.

The amide groups of polypeptides are strongly chromatophoric in IR absorption and these groups give rise to strong characteristic bands. The correlation between these characteristic bands and conformations

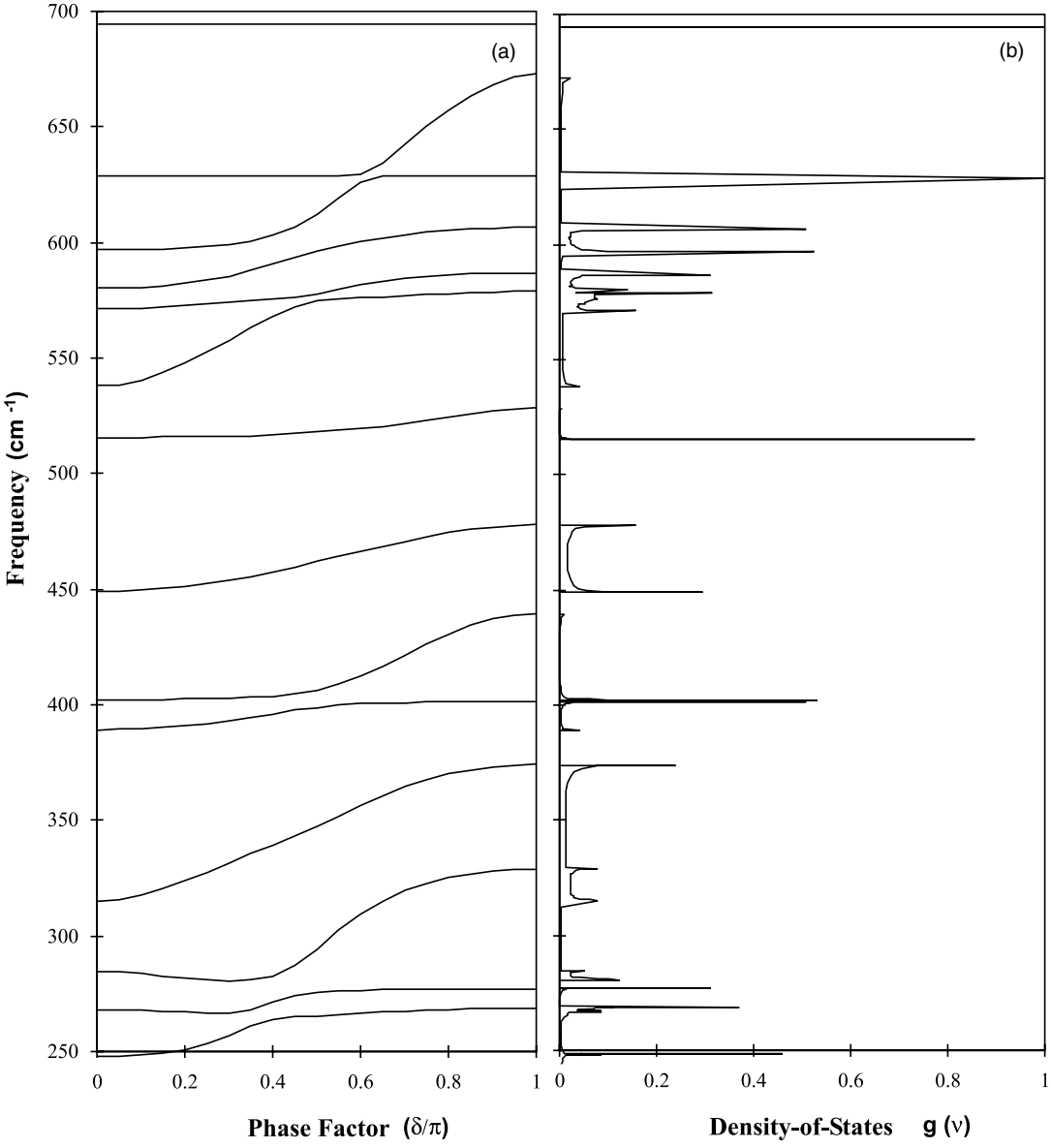

Fig. 4. (a) Dispersion curves (700–250 cm^{-1}). (b) Density of states (700–250 cm^{-1}).

have been found to be extremely useful for structural diagnosis of polypeptides and fibrous proteins [22–24]. A comparison of the amide modes of various conformations of PBLA (left-handed α helix, right-handed α helix, β sheet and ω conformation) is given in Table 3. Considerable differences in these modes are seen especially for amides I and III indicating different conformations having different hydrogen bond strengths. A comparison of amide modes in the β form of different polypeptides are also shown in Table 4. The differences reflect the effect of side chains on the amide mode frequencies. It is clear that the side-chain conformation plays an important role in determining the energy as well as the dispersive behaviour of various modes. Amide III, V, VII are indicative of the main-chain conformation, but to a limited extent these modes are also found to be sensitive to the side-chain conformation as well [7,13,14,25].

In all the forms of PBLA the amide modes except amide A and I are dispersive in nature. The amide A band arising due to the N–H stretching vibration is localised in nature. This frequency is calculated at

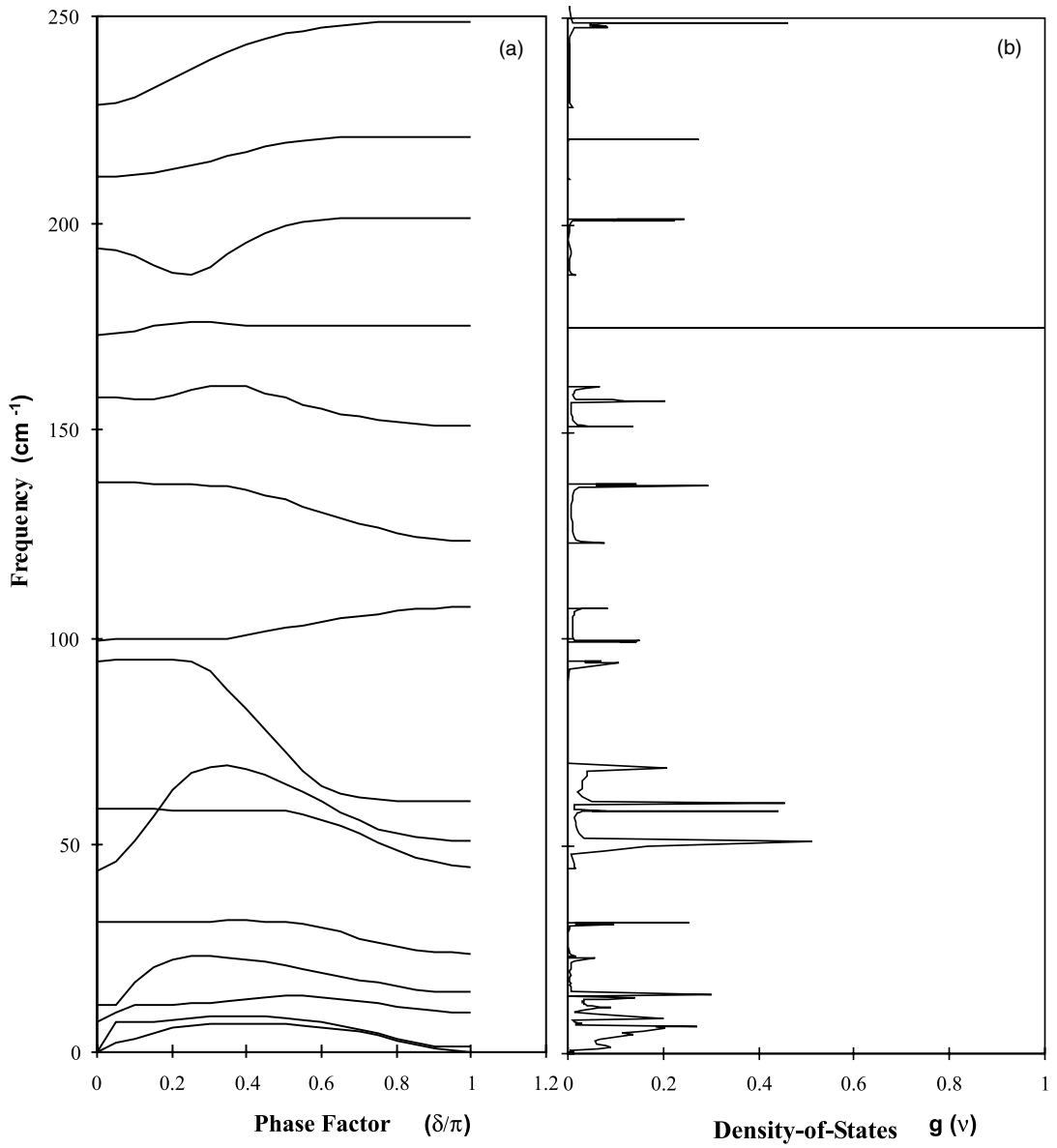

Fig. 5. (a) Dispersion curves (below 250 cm^{-1}). (b) Density of states (below 250 cm^{-1}).

3287 cm^{-1} for β-PBLA, and is in the same region as in β-PLV (3290 cm^{-1}).

The crystalline two-dimensional unit cell of a β sheet polypeptide contains four peptide groups. Therefore, four degenerate amide I vibrations of the peptide groups are expected on account of the coupling of the peptide groups through interchain hydrogen bonding interactions. Using the Krimm and Abe [26] perturbation theory, Frushour and Koenig have calculated four splitted amide I frequencies for various β sheet polypeptides. This perturbation treatment on the amide I vibration suggests a relationship between frequency splitting of this mode and the crystalline field structure. In the case of β-PBLA Frushour and Koenig have reported observed frequencies at 1636 and 1690 cm^{-1} in IR and at 1670 cm^{-1} in the Raman. The fourth component was not observed. Since our calculations are for an isolated chain, we obtain only one calculated amide I frequency at 1636 cm^{-1} which is assigned to the strong peak observed at 1636 cm^{-1} in IR.

The amide II consists of N–H in-plane bending and C=N stretching modes. This mode is also localised in the amide group and as such not very sensitive to the conformation of the chain. The amide II, assigned to

Table 1
Internal co-ordinates and force constants (md/Å)[a]

Internal co-ordinates	Force constants
ν(N==C)	5.810
ν(N–H)	5.430
ν(N–Cα)	3.450
ν(Cα–Hα)	4.147
ν(Cα–C)	2.100
ν(C==O)	8.340
ν(Cα–Cβ)	3.440
ν(Cβ–Cγ)	3.000
ν(Cβ–Hβα)	4.220
ν(Cβ–Hββ)	4.220
ν(Cγ==Oγ)	10.55
ν(Cγ–Oδ)	4.350
ν(Cε–Oδ)	4.240
ν(Cε–Hεα)	4.250
ν(Cε–Hεβ)	4.250
ν(Cη1–Cη2)	5.440
ν(Cη2–Cη3)	5.380
ν(Cη3–Cη4)	5.440
ν(Cη4–Cη5)	5.380
ν(Cη5–Cη6)	5.440
ν(Cη6–Cη1)	5.380
ν(Cη2–Hη2)	4.710
ν(Cη3–Hη3)	4.710
ν(Cη4–Hη4)	4.710
ν(Cη5–Hη5)	4.710
ν(Cη6–Hη6)	4.710
ϕ(C==N–Cα)	0.240(0.35)
ϕ(C==N–H)	0.385(0.50)
ϕ(Cα–C==O)	0.250(0.60)
ϕ(N==C–Cα)	0.210(0.60)
ϕ(O==C==N)	0.350(0.90)
ϕ(Cα–N–H)	0.340(0.40)
ϕ(N–Cα–Hα)	0.360(0.50)
ϕ(N–Cα–C)	0.530(0.50)
ϕ(C–Cα–Hα)	0.320(0.48)
ϕ(Hα–Cα–Cβ)	0.410(0.48)
ϕ(N–Cα–Cβ)	0.490(0.50)
ϕ(C–Cα–Cβ)	0.450(0.30)
ϕ(Cα–Cβ–Cγ)	0.480(0.40)
ϕ(Cα–Cβ–Hβα)	0.450(0.30)
ϕ(Cγ–Cβ–Hβα)	0.450(0.30)
ϕ(Hββ–Cβ–Hβα)	0.327(0.35)
ϕ(Cα–Cβ–Hββ)	0.450(0.30)
ϕ(Cγ–Cβ–Hββ)	0.450(0.30)
ϕ(Cβ–Cγ–Oδ)	0.330(0.50)
ϕ(Oδ–Cε–Hεβ)	0.400(0.25)
ϕ(Cβ–Cγ–Oγ)	0.270(0.58)
ϕ(Oδ–Cγ==Oγ)	0.330(0.80)
ϕ(Cγ–Oδ–Cε)	0.400(0.45)
ϕ(Oδ–Cε–Hεα)	0.400(0.25)
ϕ(Cη1–Cε–Hεβ)	0.425(0.30)
ϕ(Hε–Cε–Hε)	0.375(0.35)
ϕ(Cη1–Cε–Hεα)	0.425(0.30)
ϕ(Cη1–Cε–Oδ)	0.280(0.28)
ϕ(Cε–Cη1–Cη2)	0.720(0.55)
ϕ(Cε–Cη1–Cη6)	0.620(0.45)
ϕ(Cη2–Cη1–Cη6)	0.655(0.60)
ϕ(Cη5–Cη6–Cη1)	0.655(0.60)
ϕ(Cη1–Cη2–Cη3)	0.655(0.60)
ϕ(Cη2–Cη3–Cη4)	0.655(0.60)
ϕ(Cη3–Cη4–Cη5)	0.655(0.60)
ϕ(Cη4–Cη5–Cη6)	0.655(0.60)
ϕ(Cη1–Cη6–Hη6)	0.367(0.30)
ϕ(Cη3–Cη2–Hη2)	0.367(0.30)
ϕ(Cη2–Cη3–Hη3)	0.367(0.30)
ϕ(Cη4–Cη3–Hη3)	0.367(0.30)
ϕ(Cη3–Cη4–Hη4)	0.367(0.30)
ϕ(Cη5–Cη4–Hη4)	0.367(0.30)
ϕ(Cη4–Cη5–Hη5)	0.367(0.30)
ϕ(Cη6–Cη5–Hη5)	0.367(0.30)
ϕ(Cη5–Cη6–Hη6)	0.367(0.30)
ω(Cγ–Oγ)	0.380
ω(Cη2–Hη2)	0.280
ω(Cη3–Hη3)	0.280
ω(Cη4–Hη4)	0.280
ω(Cη5–Hη5)	0.280
ω(Cη6–Hη6)	0.280
ω(N–H)	0.150
ω(C==O)	0.390
τ(N–Cα)	0.010
τ(Cα–C)	0.040
τ(Cα–Cβ)	0.030
τ(Cβ–Cγ)	0.025
τ(Cγ–Oδ)	0.032
τ(Cε–Oδ)	0.030
τ(Cε–Cη1)	0.025
τ(Cη1–Cη2)	0.036
τ(Cη2–Cη3)	0.032
τ(Cη3–Cη4)	0.036
τ(Cη4–Cη5)	0.032
τ(Cη5–Cη6)	0.036
τ(Cη6–Cη1)	0.032
τ(N==C)	0.030

[a] Note: ν, ϕ, ω and τ denote stretch, angle bend, wag and torsion respectively. Nonbonded force constants are given in parenthesis.

1533 cm^{-1}, is calculated at 1529 cm^{-1}. In α_l-PBLA it is observed at 1556 cm^{-1}.

The amide III bands appear at 1261 and 1296 cm^{-1} in case of β and α forms respectively. The magnitude of dispersion is same in both the cases, but in the β form the frequency increases with δ whereas in α it decreases. The difference in frequencies as well as dispersion trends could be due to the different strength and nature of hydrogen bonding and main-chain conformations in the two forms of PBLA.

The amide V mode is very sensitive to the backbone conformation [22]. Since it is essentially N–H wagging motion, the strength of the hydrogen bond determines the frequency as well as its dispersion. For β sheet structures, the amide V appears generally in the region of 700 cm^{-1} (Table 5). The calculated value at 714 cm^{-1}

Table 2
Backbone modes[a]

Calculated	Observed (R)	Observed (IR)	Assignment (% PED) at ($\delta = 0$)		Calculated	Observed (R)	Observed (IR)	Assignment (% PED at $\delta = \pi$)	
3287		3290*	ν(N–H)(100)	Amide A	3287		3290*	ν(N–H)(100)	Amide A
1636		1636	ν(C=O)(62) + ν(N=C)(27)	Amide I	1636		1636	ν(C=O)(63) + ν(N=C)(24)	Amide I
1529		1533	ϕ(C=N–H)(36) + ϕ(Cα–N–H)(33) + ν(N=C)(16) + ν(N–Cα)(8)	Amide II	1525		1533	ϕ(C=N–H)(35) + ϕ(Cα–N–H)(33) + ν(N=C)(17) + ν(N–Cα)(7)	Amide II
740			ω(N–H)(45) + ω(C=O)(25) + ϕ(N–Cα–C)(6)	Amide V	714	702	697	ω(N–H)(49) + ω(C=O)(16) + ϕ(O=C=N)(7)	Amide V

[a] All frequencies are in cm^{-1}.
* Data quoted from Ref. [14].

($\delta = \pi$) is identified with 697 cm^{-1} in IR whereas for the α form it is observed at 677 cm^{-1}. This mode shows similar dispersive trends in both α and β forms.

To check the validity of the force constants and assignments, N-deuterated frequencies of β-PBLA were calculated. Since the N-deuterated spectra of β-PBLA is not available, the amide shifts were compared with the shifts reported in similar polypeptides e.g. β-PLV [14]. These results are shown in Table 5 wherein the N-deuterated shifts of PBLA are shown along with the corresponding shifts for β-PLV indicating correct assignments.

The backbone related Hα bending mode is calculated at 1335 cm^{-1} and is identified with the observed peak at 1337 cm^{-1}. This mode shows negligible dispersion and is not affected by the chain conformation because in the α form also it is observed at 1336 cm^{-1}. Another skeletal mode having contributions from (N–Cα) and (Cα–C) stretching modes is calculated at 1124 cm^{-1} and observed at 1125 cm^{-1} in the β sheet. The same mode is observed at 1127 cm^{-1} in the α form and shows small dispersion but with opposite trend.

3.2. Side-chain modes

The side chain consists of two methylene groups at β and ε positions attached with Cγ=Oγ and Cγ–Oδ–Cε parts of the ester group and terminating with a phenyl ring at η position. Most of the modes due to $C\beta H_2$ group in the side chain are mixed with the vibrations of the backbone via Cα atom and hence do not appear as pure side-chain modes.

The ring modes are localised and are nondispersive in nature. A comparison of calculated and the observed ring frequencies are given in Table 6 and are matched with the reported data of α_l-PBLA [7]. Even in other polymers where phenyl ring is present these modes are observed at about the same values, e.g. poly(γ-benzyl-L-glutamate), polystyrene [27], poly(L-phenyl alanine) [28], etc.

The observed and calculated frequencies at $\delta = 0$ and $\delta = \pi$ for side-chain modes other than the ring modes are given in Table 7. The stretch of ester bond (C=O) is calculated at 1734 cm^{-1} and observed at 1736 cm^{-1}. This value is much higher than the amide I (C=O) which is observed at a lower frequency (1636 cm^{-1}) due to the C=O···N–H hydrogen bonding. The scissoring of $C\varepsilon H_2$ methylene group, placed next to the benzene ring, calculated at 1456 cm^{-1} is observed at the same value. Another frequency calculated at 1423 cm^{-1} mainly comprises of scissoring mode of $C\beta H_2$ group adjacent to Cγ–Oγ part of the ester group. These two modes show localised group character and are also observed at the same value in the α form. $C\varepsilon H_2$ rocking mode is calculated at 910 cm^{-1} and is matched to the observed IR peak at the same value. $C\beta H_2$ rocking is at 982 cm^{-1} at $\delta = 0$

Table 3
Amide modes of various conformations of PBLA

Modes	α_l-helices	α_r-helices	β-sheet	ω-helices
Amide A	3300	3296	3287	3298
Amide I	1666	1659	1636	1677
Amide II	1556	1553	1533	1538
Amide III	1298	–	1265	1299
Amide IV	664	658	630	–
Amide V	616	602	697	621
Amide VI	616	602	571	668
Amide VII	112	112	151	98

Table 4
Comparison of various amide modes in different β pleated polypeptides

	PBLA		PLG		PLS		PLG I		PLV		PLA	
	$\delta = 0$	$\delta = \pi$	$\delta = 0$	$\delta = \pi$	$\delta = 0$	$\delta = \pi$	$\delta = 0$	$\delta = \pi$	$\delta = 0$	$\delta = \pi$	$\delta = 0$	$\delta = \pi$
Amide A	3287[a]	3287[a]	3230	3230	3318	3318	3300	3300	3290	3290	3283	3283
Amide I	1636	1636	1624	1624	1628	1628	1690	1695	1638	1638	1695	1634
Amide II	1533	1533	1560	1560	1537	1528	1514	1524	1545	1545	1524	1524
Amide III	1265	1237[a]	1259	1241[a]	249	1239	1240	1220	1228	1228	1224	1241
Amide IV	–	–	549[a]	–	533	773	628	773	584	684	594	657
Amide V	697	697	705	705	713	685	699	700	715	715	622	705
Amide VI	–	–	653	653	625[a]	647	618	600	615	628	594	657
Amide VII	158	–									247	–

[a] These frequencies are the calculated ones.

Table 5
Shifts on N-deuteration[a]

Assignments	β-PBLA		β-PLV	
	Frequency of the N–H mode	Frequency of the N–D mode	Frequency of the N–H mode	Frequency of the N–D mode
Amide A	3287	2399	3289	2399
Amide II	1529	1410	1537	1380
Amide III	1261	1019	1256	1023
Amide V	714	547	708	536

[a] All frequencies are in cm^{-1}.

and 970 cm^{-1} at $\delta = \pi$. A nondispersive pure side-chain mode calculated at 814 cm^{-1} in case of β-PBLA, is observed at 820 cm^{-1} in case of α-PBLA.

The side-chain modes which also have contributions from the backbone are considered as mixed modes and given in Table 8. These are the modes where maximum dispersion is seen as they are coupled along the chain. Such modes are discussed in the next subsection.

3.3. Dispersion curves

Since α- and β-PBLA have the same chemical repeat unit but different backbone conformation, it is interesting to compare the dispersion curves of these two systems. The modes above 1400 cm^{-1} have nondispersive character and are calculated at about the same values in all three forms of PBLA. These modes include ν(C–H), ν(N–H), scissoring of $C\beta H_2$ and $C\varepsilon H_2$ groups and ν(Cη–Cη) in the ring.

The dispersion curves for α- and ω-PBLA are similar in shape and extent because the ω (4-fold) helix is a distorted α (3.6-fold) helix and they also have similar 13 member H-bonded rings. In comparison to α- and ω-PBLA, the amount of dispersion in β-PBLA is generally found to have greater values, for example, the junction mode primarily consisting of ν(N–Cα) appears at 1110 cm^{-1} near the zone centre. This mode is repelled by the approaching mode (1068 cm^{-1}) at $\delta = 0.70\pi$ and gets dispersed in similar fashion as in α-PBLA, but the net dispersion for β-PBLA is more than that of α- and ω-PBLA.

Table 6
Ring modes

Calculated	Observed		Assignment (% PED at $\delta = 0$)	Calculated	Observed		Assignment (% PED at $\delta = \pi$)
	(R)	(IR)			(R)	(IR)	
3051		3066*	ν(Cη4–Hη4)(26) + ν(Cη3–Hη3)(19) + ν(Cη5–Hη5)(19) + ν(Cη2–Hη2)(18) + ν(Cη6–Hη6)(17)	3051		3066*	ν(Cη4–Hη4)(26) + ν(Cη3–Hη3)(19) + ν(Cη5–Hη5)(19) + ν(Cη2–Hη2)(18) + ν(Cη6–Hη6)(17)
3046		3034*	ν(Cη2–Hη2)(29) + ν(Cη5–Hη5)(25) + ν(Cη6–Hη6)(24) + ν(Cη3–Hη3)(21)	3046		3034*	ν(Cη2–Hη2)(29) + ν(Cη5–Hη5)(25) + ν(Cη6–Hη6)(24) + ν(Cη3–Hη3)(21)
3045		3034*	ν(Cη6–Hη6)(33) + ν(Cη2–Hη2)(29) + ν(Cη3–Hη3)(18) + ν(Cη5–Hη5)(14)	3045		3034*	ν(Cη6–Hη6)(33) + ν(Cη2–Hη2)(29) + ν(Cη3–Hη3)(18) + ν(Cη5–Hη5)(14)
3043		3034*	ν(Cη4–Hη4)(68) + ν(Cη5–Hη5)(15) + ν(Cη3–Hη3)(14)	3043		3034*	ν(Cη4–Hη4)(68) + ν(Cη5–Hη5)(15) + ν(Cη3–Hη3)(14)
3042		3034*	ν(Cη5–Hη5)(27) + ν(Cη3–Hη3)(26) + ν(Cη6–Hη6)(23) + ν(Cη2–Hη2)(23)	3042		3034*	ν(Cη5–Hη5)(27) + ν(Cη3–Hη3)(26) + ν(Cη6–Hη6)(23) + ν(Cη2–Hη2)(23)
1619	1611	1627*	ν(Cη2–Cη3)(20) + ν(Cη4–Cη5)(9) + ν(Cη6–Cη1)(19) + ν(Cη1–Cη2)(8) + ϕ(Cη1–Cη2–Hη2)(5)	1619	1611		ν(Cη2–Cη3)(20) + ν(Cη4–Cη5)(19) + ν(Cη6–Cη1)(9) + ν(Cη1–Cη2)(8) + ϕ(Cη1–Cη2–Hη2)(5)
1598	1589	1596*	ν(Cη1–Cη2)(26) + ν(Cη6–Cη1)(25) + ν(Cη5–Cη6)(9) + ν(Cη3–C4η4)(9)	1598	1589		ν(Cη1–Cη2)(26) + ν(Cη6–Cη1)(25) + ν(Cη5–Cη6)(9) + ν(Cη3–Cη4)(9)
1583		1576*	ν(Cη5–Cη6)(24) + ν(Cη3–Cη4)(23) + ν(Cη4–Cη5)(14) + ν(Cη2–Cη3)(13) + zν(Cη6–Cη1)(7) + ν(Cη1–Cη2)(7)	1583		1576*	ν(Cη5–Cη6)(24) + ν(Cη3–Cη4)(23) + ν(Cη4–Cη5)(14) + ν(Cη2–Cη3)(13) + ν(Cη6–Cη1)(7) + ν(Cη1–Cη2)(7)
1503	1499	1500	ν(Cη3–Cη4)(10) + ν(Cη5–Cη6)(10) + ϕ(Cη2–Cη3–Hη3)(9) + ϕ(Cη6–Cη5–Hη5)(9) + ϕ(Cη4–Cη3–Hη3)(9) + ϕ(Cη4–Cη5–Hη5)(8) + ν(Cη6–Cη1)(7) + ν(Cη1–Cη2)(7) + ϕ(Cη5–Cη6–Hη6)(5) + ν(Cε–Cη1)(5)	1503	1499	1500	ν(Cη3–Cη4)(10) + ν(Cη5–Cη6)(10) + ϕ(Cη2–Cη3–Hη3)(9) + ϕ(Cη6–Cη5–Hη5)(9) + ϕ(Cη4–Cη3–Hη3)(9) + ϕ(Cη4–Cη5–Hη5)(8) + ν(Cη6–Cη1)(7) + ν(Cη1–Cη2)(7) + ϕ(Cη5–Cη6–Hη6)(5) + ν(Cε–Cη1)(5)
1467		1456*	ϕ(Cη5–Cη4–Hη4)(11) + ϕ(Cη3–Cη4–Hη4)(11) + γ(Cη4–Cη5)(10) + ν(Cη2–Cη3)(9) + ϕ(Hε–Cε–Hε)(6) + ϕ(Cη4–Cη5–Hη5)(5)	1467			ϕ(Cη5–Cη4–Hη4)(11) + ϕ(Cη3–Cη4–Hη4)(11) + γ(Cη4–Cη5)(10) + ν(Cη2–Cη3)(9) + ϕ(Hε–Cε–Hε)(6) + ϕ(Cη4–Cη5–Hη5)(5)
1322		1336*	ϕ(Cη1–Cη6–Hη6)(13) + ϕ(Cη5–Cη6–Hη6)(13) + ν(Cε–Cη1)(11) + ϕ(Cη1–Cη2–Hη2)(8) + ν(Cε–O)(7) + ϕ(Cη1–Cε–Hε)(7) + ν(Oδ–Cε–Hε)(6)	1322			ϕ(Cη1–Cη6–Hη6)(13) + ϕ(Cη5–Cη6–Hη6)(13) + ν(Cε–Cη1)(11) + ϕ(Cη1–Cη2–Hη2)(8) + ν(Cε–O)(7) + ϕ(Cη1–Cε–Hε)(7) + ν(Oδ–Cε–Hε)(6)
1187	1184*		ϕ(Cη3–Cη4–Hη4)(15) + ϕ(Cη5–Cη4–Hη4)(13) + ϕ(Cη4–Cη5–Hη5)(12) + (ϕ(Cη2–Cη3–Hη3)(10) + ϕ(Cη4–Cη3–Hη3)(10) + ϕ(Cη6–Cη5–Hη5)(10)	1187			ϕ(Cη3–Cη4–Hη4)(15) + ϕ(Cη5–Cη4–Hη4)(13) + ϕ(Cη4–Cη5–Hη5)(12)ϕ(Cη2–Cη3–Hη3)(10) + ϕ(Cη4–Cη3–Hη3)(10) + ϕ(Cη6–Cη5–Hη5)(10)
1158		1166*	ϕ(Cη2–Cη3–Hη3)(13) + ϕ(Cη6–Cη5–Hη5)(12) + γ(Cη4–Cη5)(10) + ν(Cη2–Cη3)(10) + ϕ(Cη4–Cη3–Hη3)(10) + ϕ(Cη1–Cη6–Hη6)(8) + ϕ(Cη4–Cη5–Hη5)(8) + ϕ(Cη5–Cη6–Hη6)(7) + ϕ(Cη1–Cη2–Hη2)(7) + ϕ(Cη3–Cη2–Hη2)(7)	1158			ϕ(Cη2–Cη3–Hη3)(13) + ϕ(Cη6–Cη5–Hη5)(12) + γ(Cη4–Cη5)(10) + ν(Cη2–Cη3)(10) + ϕ(Cη4–Cη3–Hη3)(10) + ϕ(Cη4–Cη5–Hη5)(8) + ϕ(Cη1–Cη6–Hη6)(8) + ϕ(Cη5–Cη6–Hη6)(7) + ϕ(Cη1–Cη2–Hη2)(7) + ϕ(Cη3–Cη2–Hη2)(7)

1017		1028*	ν(Cη6–Cη1)(13) + ν(Cη1–Cη2)(13) + ϕ(Cη5–Cη6–Cη1)(9) + ϕ(Cη4–Cη5–Cη6)(9) + ϕ(Cη2–Cη3–Cη4)(9) + ϕ(Cη1–Cη2–Cη3)(8) + ϕ(Cη4–Cη5–Hη5)(6) + ϕ(Cη1–Cη6–Hη6)(6) + ϕ(Cη1–Cη2–Hη2)(6) + ϕ(Cη4–Cη3–Hη3)(6)	1017			ν(Cη6–Cη1)(13) + ν(Cη1–Cη2)(13) + ϕ(Cη5–Cη6–Cη1)(9) + ϕ(Cη4–Cη5–Cη6)(9) + ϕ(Cη2–Cη3–Cη4)(9) + ϕ(Cη1–Cη2–Cη3)(8) + ϕ(Cη4–Cη5–Hη5)(6) + ϕ(Cη1–Cη6–Hη6)(6) + ϕ(Cη1–Cη2–Hη2)(6) + ϕ(Cη4–Cη3–Hη3)(6)
1010	1006		ν(Cη5–Cη6)(28) + ν(Cη3–Cη4)(28) + ν(Cη2–Cη3)(9) + ν(Cη4–Cη5)(9)	1010	1006		ν(Cη5–Cη6)(28) + ν(Cη3–Cη4)(28) + ν(Cη2–Cη3)(9) + ν(Cη4–Cη5)(9)
1009		996*	ω(Cη4–Hη4)(29) + ω(Cη3–Hη3)(22) + ω(Cη5–Hη5)(21) + ω(Cη6–Hη6)(8) + ω(Cη2–Hη2)(8)	1009		996*	ω(Cη4–Hη4)(29) + ω(Cη3–Hη3)(22) + ω(Cη5–Hη5)(21) + ω(Cη6–Hη6)(8) + ω(Cη2–Hη2)(8)
953	952	951*	ω(Cη5–Hη5)(22) + ω(Cη6–Hη6)(21) + ω(Cη2–Hη2)(21) + ω(Cη3–Hη3)(20) + τ(Cη5–Cη6)(6)	953	952	951*	ω(Cη6–Hη6)(21) + ω(Cη5–Hη5)(21) + ω(Cη2–Hη2)(21) + ω(Cη3–Hη3)(20) + τ(Cη5–Cη6)(6)
814	832		ν(Cε–Cη1)(26) + ϕ(Cη3–Cη4–Cη5)(17) + ν(Cη6–Cη1)(15) + ν(Cη1–Cη2)(10) + ϕ(Cη2–Cη3–Cη4)(6) + ϕ(Cη4–Cη5–Cη6)(5)	813	832	803	ν(Cε–Cη1)(25) + ϕ(Cη3–Cη4–Cη5)(16) + ν(Cη6–Cη1)(13) + ν(Cη1–Cη2)(9) + ϕ(Cη2–Cη3–Cη4)(6) + ϕ(Cη4–Cη5–Cη6)(5)
771	760	750	ω(Cη6–Hη6)(23) + ω(Cη5–Hη5)(22) + ω(Cη3–Hη3)(22) + ω(Cη2–Hη2)(19)	771	760	750	ω(Cη6–Hη6)(23) + ω(Cη5–Hη5)(22) + ω(Cη3–Hη3)(22) + ω(Cη2–Hη2)(19)
695		698*	ω(Cη4–Hη4)(32) + ω(Cη3–Hη3)(23) + ω(Cη5–Hη5)(23) + ω(Cη6–Hη6)(9) + ω(Cη2–Hη2)(7)	695			ω(Cη4–Hη4)(32) + ω(Cη3–Hη3)(23) + ω(Cη5–Hη5)(23) + ω(Cη6–Hη6)(9) + ω(Cη2–Hη2)(7)
629	646	630	ϕ(Cη4–Cη5–Cη6)(20) + ϕ(Cη1–Cη2–Cη3)(19) + ϕ(Cη2–Cη3–Cη4)(15) + ϕ(Cη5–Cη6–Cη1)(15) + ϕ(Cη1–Cη2–Hη2)(17)	673	646	630	ϕ(Cη4–Cη5–Hη6)(20) + ϕ(Cη1–Cη2–Cη3)(19) + ϕ(Cη2–Cη3–Cη4)(15) + ϕ(Cη5–Cη6–Cη1)(15) + ϕ(Cη1–Cη2–Hη2)(17)
268			τ(Cη5–Cη6)(20) + τ(Cη2–Cη3)(16) + τ(Cη3–Cη4)(7) + ϕ(C–Cα–Cβ)(6)	277			τ(Cη2–Cη3)(15) + τ(Cη5–Cη6)(15) + τ(Cε–Cη1)(10) + τ(Cη4–Cη5)(7) + τ(Cη1–Cη2)(6) + ϕ(Cα–C==O)(6)

* Data quoted from Ref. [7].

Table 7
Side-chain modes

Calculated	Observed		Assignment (% PED at $\delta = 0$)	Calculated	Observed		Assignment (% PED at $\delta = \pi$)
	(R)	(IR)			(R)	(IR)	
2965			ν(Cε–Hεα)(50) + ν(Cε–Hεβ)(49)	2965			ν(Cε–Hεα)(50) + ν(Cε–Hεβ)(49)
2893			ν(Cε–Hεβ)(50) + ν(Cε–Hεα)(49)	2893			ν(Cε–Hεβ)(50) + ν(Cε–Hεα)(49)
2890			ν(Cβ–Hβα)(50) + ν(Cβ–Hββ)(50)	2890			ν(Cβ–Hβα)(50) + ν(Cβ–Hββ)(50)
1734	1734	1736	ν(Cγ=Oγ)(82) + ν(Cγ–Oδ)(7)	1734	1734	1736	ν(Cγ=O)(82) + ν(Cγ–O)(7)
1456	1459	1455	ϕ(Hε–Cε–Hε)(71) + ϕ(Cη1–Cε–Hεβ)(5)	1456	1459	1455	ϕ(Hε–Cε–Hε)(71) + ϕ(Cη1–Cε–Hεβ)(5)
1423	1418	1412	ϕ(Hβ–Cβ–Hβ)(70) + ϕ(Cα–Cβ–Hββ)(10) + ϕ(Cα–Cβ–Hβα)(9)	1422	1418	1412	ϕ(Hβ–Cβ–Hβ)(70) + ϕ(Cα–Cβ–Hββ)(10) + ϕ(Cα–Cβ–Hβα)(9)
1365	1360	1356	ν(Cε–O)(14) + ϕ(Cη1–Cε–Hεβ)(11) + ν(Cε–Cη1)(10) + ϕ(Cη1–Cε–Hε)(9) + ϕ(Oδ–Cε–Hεβ)(7) + ϕ(Oδ–Cε–Hεα)(7) + ϕ(Cη–Cη–Hη)(35)	1365	1360	1356	ν(Cε–O)(14) + ϕ(Cη1–Cε–Hεβ)(11) + ν(Cε–Cη1)(10) + ϕ(Cη1–Cε–Hε)(9) + ϕ(Oδ–Cε–Hε)(7) + ϕ(Oδ–Cε–Hε)(7) + ϕ(Cη3–Cη2–Hη2)(7)
1228			ν(Cγ–Oδ)(32) + γ(Cβ–Cγ)(20) + ν(Cε–Cη1)(10)	1227			ν(Cγ–O)(29) + ν(Cβ–Cγ)(18) + ν(Cε–Cη1)(10)
1198			ν(Cγ–O)(14) + ν(Cβ–Cγ)(11) + ν(Cε–Cη1)(10) + ϕ(Cη–Cη–Hη)(20) + ϕ(Cη1–Cε–Hεβ)(6) + ϕ(Oδ–Cε–Hεα)(5)	1198			ν(Cγ–O)(14) + ν(Cβ–Cγ)(12) + ν(Cε–Cη1)(9) + ϕ(Cη3–Cη2–Hη2)(7) + ϕ(Cη1–Cε–Hεβ)(6) + ϕ(Oδ–Cε–Hεα)(5)
1167	1161	1162	ϕ(Cη1–Cε–Hεα)(26) + ϕ(Cη1–Cε–Hεβ)(26) + ϕ(Oδ–Cε–Hεβ)(18) + ϕ(Oδ–Cε–Hεα)(18)	1167	1161	1162	ϕ(Cη1–Cε–Hεα)(26) + ϕ(Cη1–Cε–Hεβ)(26) + ϕ(Oδ–Cε–Hεβ)(18) + ϕ(Oδ–Cε–Hεα)(18)
910	911	910	ϕ(Oδ–Cε–Hεβ)(18) + ϕ(Oδ–Cε–Hεα)(14) + ϕ(Cη1–Cε–Hεα)(12) + ϕ(Cη1–Cε–Hεβ)(10) + τ(Cε–Oδ)(6) + ν(Cβ–Cγ)(5)	907	911	910	ϕ(Oδ–Cε–Hεβ)(18) + ϕ(Oδ–Cε–Hεα)(15) + ϕ(Cη1–Cε–Hεα)(12) + ϕ(Cη1–Cε–Hεβ)(11) + τ(Cε–Oδ)(6)
211			τ(Cη–Cη)(41) + τ(Cε–Cη1)(12) + ϕ(Cγ–Oδ–Cε)(11)	221			ϕ(Cγ–Oδ–Cε)(15) + τ(Cε–Cη1)(13) + τ(Cη6–Cη1)(9) + ϕ(Oδ–Cγ–Oγ)(8) + τ(Cγ–Oδ)(7) + τ(Cη3–Cη4)(6)
173			ϕ(Cγ–Oδ–Cε)(13) + τ(Cη–Cη)(41) + τ(Cγ–Oδ)(7) + τ(Cε–Cη1)(7) + τ(Cβ–Cγ)(5)	175			τ(Cβ–Cγ)(14) + τ(Cη1–Cη2)(13) + ϕ(Cγ–Oδ–Cε)(9) + τ(Cη4–Cη5)(9) + τ(Cη6–Cη1)(9) + τ(Cε–Cη1)(7) + τ(Cη3–Cη4)(6)
31			τ(Cγ–Oδ)(13) + τ(Cα–Cβ)(13) + τ(Cε–Cη1)(11) + τ(Cη–Cη)(27)	24			τ(Cα–Cβ)(29) + τ(Cγ–Oδ)(8) + τ(Cη2–Cη3)(6) + τ(Cε–Cη1)(6)
7			τ(Cα–Cβ)(28) + τ(Cβ–Cγ)(19) + ω(Cγ–O)(8) + τ(Cε–Oδ)(8) + τ(Cη–Cη)(23)	9			τ(Cβ–Cγ)(22) + τ(Cα–Cβ)(21) + τ(Cη2–Cη3)(10) + τ(Cη5–Cη6)(8) + τ(Cε–Oδ)(7) + ω(Cγ–O)(6)

Table 8
Mixed modes

Calculated	Observed		Assignment (% PED at $\delta = 0$)	Calculated	Observed		Assignment (% PED at $\delta = \pi$)
	(R)	(IR)			(R)	(IR)	
2967			ν(Cα–Hα)(53) + ν(Cβ–Hββ)(26) + ν(Cβ–Hβα)(21)	2967			ν(Cα–Hα)(54) + ν(Cβ–Hββ)(25) + ν(Cβ–Hβα)(21)
2957			ν(Cα–Hα)(49) + ν(Cβ–Hβα)(28) + ν(Cβ–Hββ)(23)	2957			ν(Cα–Hα)(49) + ν(Cβ–Hβα)(28) + ν(Cβ–Hββ)(23)
1383	1383	1385	ν(Cα–Cβ)(16) + ϕ(Cγ–Cβ–Hβα)(14) + ϕ(Hα–Cα–Cβ)(12) + ϕ(Cγ–Cβ–Hββ)(10) + ϕ(N–Cα–Hα)(10) + ϕ(Cα–Cβ–Hβα)(8) + ϕ(Cα–Cβ–Hββ)(8) + ν(Cβ–Cγ)(7)	1383	1383	1385	ν(Cα–Cβ)(17) + ϕ(Cγ–Cβ–Hβα)(14) + ϕ(Hα–Cα–Cβ)(12) + ϕ(Cγ–Cβ–Hββ)(11) + ϕ(N–Cα–Hα)(9) + ϕ(Cα–Cβ–Hβα)(9) + ϕ(Cα–Cβ–Hββ)(8) + ν(Cβ–Cγ)(8)
1335	1337		ϕ(Hα–Cα–Cβ)(35) + ϕ(N–Cα–Hα)(20) + ϕ(Cγ–Cβ–Hβα)(9) + ϕ(Cα–Cβ–Hββ)(9) + ϕ(Cγ–Cβ–Hββ)(8)	1332	1337		ϕ(Hα–Cα–Cβ)(39) + ϕ(N–Cα–Hα)(19) + ϕ(Cγ–Cβ–Hββ)(9) + ϕ(Cγ–Cβ–Hβα)(9) + ϕ(Cα–Cβ–Hββ)(8)
1287	1288	1298	ϕ(C–Cα–Hα)(38) + ϕ(N–Cα–Hα)(17) + ν(Cα–C)(8) + ϕ(Hα–Cα–Cβ)(7) + ϕ(Cα–Cβ–Hβα)(6) + ν(Cα–Cβ)(5)	1282	1288	1298	ϕ(C–Cα–Hα)(30) + ϕ(N–Cα–Hα)(14) + ν(Cα–C)(13) + ν(C═O)(7) + ϕ(Hα–Cα–Cβ)(5) + ϕ(Cα–Cβ–Hβα)(5)
1261	1254	1265	ν(N═C)(31) + ν(Cα–C)(13) + ϕ(Cα–N–H)(9) + ν(C═O)(8) + ϕ(C═N–H)(5) amide III	1240	1237		ν(N═C)(22) + ν(C═O)(9) + ν(Cα–C)(9) + ϕ(Cγ–Cβ–Hββ)(8) + ϕ(Cα–Cβ–Hβα)(7) + ν(N–Cα)(6) + ϕ(Cα–N–H)(5) amide III
1209	1217	1216	ϕ(Cγ–Cβ–Hβα)(15) + ϕ(Cγ–Cβ–Hββ)(13) + ϕ(Cα–Cβ–Hβα)(12) + ϕ(Cα–Cβ–Hββ)(11) + ϕ(C–Cα–Hα)(8) + ν(Cα–C)(6)	1208	1217	1216	ϕ(C–Cα–Hα)(16) + ϕ(Cγ–Cβ–Hβα)(12) + ϕ(Cγ–Cβ–Hββ)(11) + ϕ(Cα–Cβ–Hα)(11) + ϕ(Cα–Cβ–Hβ)(10) + ϕ(N–Cα–Hα)(7) + ν(N═C)(7)
1124	1125		ν(N–Cα)(57) + ν(Cα–C)(12) + ϕ(N–Cα–Hα)(6)1120	1115			ν(Cα–Cβ)(49) + ν(N–Cα)(17) + ϕ(Cα–Cβ–Hβα)(7) + ϕ(Hα–Cα–Cβ)(5)
1110	1115		ν(Cα–Cβ)(60) + ϕ(Cα–Cβ–Hβα)(7)	1068			ν(Cη–Cη)(36) + ϕ(Cη–Cη–Hη)(16) + ν(Cε–O)(9)
1068	1081	1080	ν(Cη–Cη)(39) + ϕ(Cη–Cη–Hη)(31) + ν(Cε–O)(7)	1056			ν(N–Cα)(42) + ν(N═C)(9) + ν(Cα–Cβ)(8) + ϕ(N–Cα–Cβ)(7)
1039	1033	1030	ν(Cε–Oδ)(54) + ν(Cβ–Cγ)(8) + ϕ(Oδ–Cε–Hεβ)(5)	1037	1033	1030	ν(Cε–O)(48) + ν(Cβ–Cγ)(8) + ν(N–Cα)(7)
982	969	975	ϕ(Cγ–Cβ–Hβα)(16) + ϕ(Cγ–Cβ–Hββ)(12) + ν(Cα–C)(12) + ϕ(Cα–Cβ–Hβα)(11) + ϕ(Cα–Cβ–Hββ)(10) + ν(C═O)(5)	970	969	975	ϕ(Cγ–Cβ–Hβα)(19) + ϕ(Cα–Cβ–Hβα)(14) + ϕ(Cα–Cβ–Hββ)(13) + ϕ(Cγ–Cβ–Hββ)(12) + ν(Cα–C)(10) + ω(Cγ–O)(5)
866	852		ω(Cη–Hη)(51) + ν(Cα–C)(10)	866	852		ω(Cη–Hη)(44) + ν(Cγ–O)(15) + ω(Cη4–Hη4)(14) + ω(Cη6–Hη6)(13) + ν(Cβ–Cγ)(12)
864			ν(Cγ–O)(13) + ν(Cα–C)(13) + ν(Cβ–Cγ)(10) + ϕ(Cα–Cβ–Hββ)(8) + ϕ(Cγ–Cβ–Hββ)(6)	858			ω(Cη–Hη)(34) + ν(Cγ–O)(9) + ν(Cα–C)(8) + ϕ(Oδ–Cε–Hεα)(6) + ν(Cβ–Cγ)(6)

(*continued on next page*)

Table 8 (*continued*)

Calculated	Observed		Assignment (% PED at $\delta = 0$)	Calculated	Observed		Assignment (% PED at $\delta = \pi$)
	(R)	(IR)			(R)	(IR)	
852			ν(Cγ–O)(15) + ν(Cβ–Cγ)(12) + ϕ(Oδ–Cε–Hεα)(9) + ω(Cη–Hη)(6) + ϕ(Oδ–Cε–Hεβ)(6)	826	814	803	ν(Cα–C)(42) + ν(Cβ–Cγ)(5) + ν(Cγ–O)(5)
597			ω(Cγ–O)(38) + ϕ(Cα–Cβ–Cγ)(6) + τ(Cε–Oδ)(5)	629	646	630	ϕ(O=C=N)(13) + ϕ(N–Cα–C)(13) + ϕ(Cα–C=O)(12) + ω(N–H)(11) + ϕ(C=N–Cα)(10) + ω(C=O)(6) amide IV
580	581		ω(Cγ–O)(28) + ϕ(Cγ–Oδ–Cε)(11) + ϕ(Cη–Cη–Cη)(12)	606			ω(C=O)(25) + ω(N–H)(12) + ϕ(N–Cα–C)(11) + ω(Cγ–O)(10) + ϕ(C–Cα–Cβ)(8) + ϕ(Cα–Cβ–Cγ)(6) amide V + VI
571			ω(C=O)(22) + ω(N–H)(22) + τ(N=C)(10) + ϕ(C–Cα–Cβ)(8) amide V + VI	587	581		ω(Cγ–O)(30) + ω(C=O)(12)
538			ϕ(O=C=N)(33) + ϕ(Cα–C=O)(24) + ϕ(N–Cα–C)(8) amide IV	579	581		ω(Cγ–O)(27) + ϕ(Cγ–Oδ–Cε)(11) + ϕ(Cη–Cη–Cη)(14)
516	501		ϕ(Oδ–Cγ–Oγ)(19) + ϕ(Cβ–Cγ–Oδ)(11) + ϕ(Cε–Cη1–Cη6)(8) + ϕ(Cα–Cβ–Cγ)(7) + ϕ(Cγ–Oδ–Cε)(7) + ϕ(N–Cα–Cβ)(5) + ϕ(Cη1–Cε–Oδ)(5)	528			ϕ(Oδ–Cγ–Oγ)(12) + ϕ(N=C–Cα)(11) + ϕ(N–Cα–Cβ)(10) + ω(C=O)(6) + ϕ(Cε–Cη1–Cη6)(5)
449	450		ϕ(Cβ–Cγ–Oγ)(32) + ϕ(Cβ–Cγ–Oδ)(9) + ϕ(Oδ–Cγ–Oγ)(7) + ϕ(N–Cα–Cβ)(7) + ω(C=O)(6) + ϕ(Cε–Cη1–Cη2)(5)	478	486		ϕ(N=C–Cα)(16) + ϕ(Cβ–Cγ–Oδ)(14) + ϕ(Oδ–Cγ–Oγ)(8) + ϕ(O=C=N)(7) + ϕ(Cε–Cη1–Cη2)(7) + ϕ(Cε–Cη1–Cη6)(7) + ϕ(Cγ–Oδ–Cε)(7)
402	407		τ(Cη–Cη)(77)	439	450		ϕ(Cβ–Cγ–Oγ)(24) + τ(N=C)(9) + ϕ(Oδ–Cγ–Oγ)(8) + ϕ(N–Cα–C)(7) + ω(C=O)(7) + ϕ(Cα–Cβ–Cγ)(5)
389			ϕ(Cε–Cη1–Cη2)(19) + ϕ(Cε–Cη1–Cη6)(12) + ϕ(Cα–Cβ–Cγ)(10) + ϕ(N–Cα–Cβ)(5)	401			τ(Cη1–Cη2)(45) + τ(Cη2–Cη3)(41) + ω(Cη2–H)(10)
315			ϕ(N–Cα–Cβ)(35) + ϕ(Oδ–Cγ–Oγ)(7) + ω(C=O)(6) + ν(Cβ–Cγ)(5)	374	371		ϕ(Cε–Cη–Cη)(26) + ϕ(Cα–Cβ–Cγ)(7) + τ(N=C)(6) + ϕ(N–Cα–C)(6) + ϕ(C–Cα–Cβ)(5)
285	276		τ(Cε–Cη1)(14) + ϕ(C–Cα–Cβ)(9) + ϕ(Cβ–Cγ–Oδ)(8) + τ(Cη–Cη)(26) + τ(Cη5–Cη6)(8) + τ(Cγ–Oδ)(7) + τ(Cα–Cβ)(6) + τ(Cη4–Cη5)(6)	329	323		ϕ(Cβ–Cγ–Oγ)(15) + ϕ(N–Cα–C)(13) + ϕ(Cβ–Cγ–Oδ)(11) + ϕ(N–Cα–Cβ)(8) + ϕ(Cε–Cη1–Cη2)(5)
248			τ(Cε–Oδ)(20) + ϕ(Cη1–Cε–Oδ)(12) + τ(Cβ–Cγ)(9) + ϕ(Cα–C=O)(6) + ϕ(C–Cα–Cβ)(6)	269	276		ϕ(Cα–C=O)(16) + τ(Cη–Cη)(20) + ϕ(O=C=N)(9) + ϕ(C–Cα–Cβ)(6)
228			ϕ(N–Cα–C)(16) + ϕ(N=C–Cα)(15) + ϕ(Cα–C=O)(13) + ϕ(Cη1–Cε–Oδ)(8) + τ(Cε–Oδ)(6)	249			τ(Cε–Oδ)(27) + ϕ(Cη1–Cε–Oδ)(16)

194	ϕ(C═N–Cα)(21) + τ(Cα–Cβ)(10) + τ(Cα–C)(7) + ϕ(Cβ–Cγ–Oγ)(7) + ϕ(O═C═N)(7) + ϕ(C═N–H)(7) + ϕ(Cα–N–H)(6) + ϕ(Cγ–Oδ–Cε)(5)	201	τ(Cβ–Cγ)(11) + τ(Cα–C)(11) + τ(Cα–Cβ)(8) + ϕ(C═N–Cα)(8) + τ(Cη–Cη)(11) + ϕ(O═C═N)(5)
158	ϕ(N═C–Cα)(13) + τ(N–Cα)(13) + τ(Cα–C)(10) + τ(Cβ–Cγ)(9) + ν(N–Cα)(6) + ϕ(N–Cα–C)(6) + ϕ(O═C═N)(5)	151	ϕ(Cγ–Oδ–Cε)(25) + ϕ(Cα–Cβ–Cγ)(16) + τ(Cγ–Oδ)(10) + τ(Cε–Oδ)(9) + ϕ(Cβ–Cγ–Oγ)(5) amide VII
138	τ(Cγ–Oδ)(17) + ϕ(Cγ–Oδ–Cε)(14) + τ(Cε–Oδ)(13) + τ(Cε–Cη1)(7)	123	τ(Cε–Oδ)(10) + ϕ(Cη1–Cε–Oδ)(9) + τ(Cα–C)(8) + τ(Cγ–Oδ)(8) + τ(Cβ–Cγ)(8) + ϕ(C–Cα–Cβ)(5) + ϕ(Cε–Cη1–Cη6)(5) + τ(N–Cα)(5)
99	τ(Cβ–Cγ)(22) + τ(Cα–C)(14) + τ(Cα–Cβ)(10) + ϕ(C–Cα–Cβ)(8)	108	τ(Cα–C)(35) + τ(N–Cα)(8) + τ(Cε–Oδ)(5)
94	ϕ(Cα–Cβ–Cγ)(15) + τ(N═C)(14) + ϕ(Cη1–Cε–Oδ)(9) + τ(Cε–Oδ)(8) + τ(Cα–C)(7)	60	τ(Cε–Cη1)(27) + τ(Cβ–Cγ)(15) + τ(Cη–Cη)(26) + τ(Cγ–Oδ)(6)
59	τ(Cε–Cη1)(29) + τ(Cβ–Cγ)(13) + τ(Cη1–Cη2)(12) + τ(Cγ–Oδ)(9) + τ(Cη6–Cη1)(8) + τ(Cη5–Cη6)(7)	51	τ(N–Cα)(15) + ϕ(C═N–Cα)(7) + τ(Cε–Cη1)(6) + τ(Cβ–Cγ)(6) + τ(N═C)(6) + ϕ(N═C–Cα)(6)
44	ϕ(Cη1–Cε–Oδ)(17) + τ(N═C)(13) + τ(Cγ–Oδ)(12) + τ(Cε–Oδ)(10) + τ(Cα–C)(8)	45	ϕ(C–Cα–Cβ)(19) + ϕ(N–Cα–Cβ)(17) + τ(Cγ–Oδ)(12) + ϕ(Cη1–Cε–Oδ)(9) + τ(Cα–C)(8) + τ(Cε–Oδ)(6)
11	τ(Cγ–Oδ)(18) + ϕ(Cα–Cβ–Cγ)(14) + τ(N═C)(10) + ϕ(C–Cα–Cβ)(6) + ϕ(Cβ–Cγ–Oδ)(5) + τ(Cα–C)(5)	14	τ(Cγ–Oδ)(26) + ϕ(Cα–Cβ–Cγ)(17) + ϕ(Cβ–Cγ–Oδ)(9) + ϕ(Cη1–Cε–Oδ)(7) + ϕ(N–Cα–Cβ)(6) + ϕ(Cγ–Oδ–Cε)(6)

Table 9
Characteristic features of dispersion curves

Frequency ($\delta = 0$)	δ^a/π	Before exchange			After exchange		
		δ^b/π	Frequency	PED	δ^b/π	Frequency	PED
Pair of modes that repel and exchange character							
1110	0.70	0.65	1074	ν(N–Cα)(39) + ν(Cα–Cβ)(14) + ν(N==C)(7)	0.75	1069	ν(Cη–Cη)(26) + ϕ(Cη–Cη–Hη)(25)+ ν((N–Cα)(12) + ν(Cε–O)(9)
1068	0.70	0.65	1067	ν(Cη–Cη)(38) + ϕ(Cη–Cη–Hη)(35)	0.75	1064	ν((N–Cα)(34)+ ν(Cη–Cη)(14)+ ϕ(Cη–Cη–Hη)(12)+ ν(Cα–Cβ)(10) + ν(N==C)(7)
629	0.60	0.55	629	ϕ(Cη–Cη–Cη)(69)+ ϕ(Cη–Cη–Hη)(17) + ν(Cη–Cη)(5)	0.65	635	ϕ(O=C=N)(20) + ϕ(Cα–C=O)(12)+ ϕ(C=N–Cα)(10) + α(C–Cα–Cβ)(9)+ ν(Cα–C)(6)
597	0.60	0.55	619	ϕ(O=C=N)(19) + ϕ(C–Cα–Cβ)(11)+ ϕ(Cα–C=O)(11)+ ϕ(C=N–Cα)(8)+ ω(C=O)(8)+ ν(Cα–C)(5)	0.65	629	ϕ(Cη–Cη–Cη)(69)+ ϕ(Cη–Cη–Hη)(17)+ ν(Cη–Cη)(5)
571	0.50	0.45	576	ϕ(Cη–Cη–Cη)(30) + ϕ(Cγ–Oδ–Cε)(9)+ ω(Cγ–O)(9)	0.55	580	ω(Cγ–O)(14) + ϕ(Cη–Cη–Cη)(14)+ ω(C=O)(12) + ω(N–H)(8)+ ϕ(N–Cα–C)(6)
538	0.50	0.45	572	ω(C=O)(19) + ω(N–H)(17)+ ω(Cγ–O)(14) + ϕ(N–Cα–C)(11)+ τ(N=C)(8)	0.55	576	ω(Cγ–O)(20) + ϕ(Cη–Cη–Cη)(18)+ ω(C=O)(9) + ω(N–H)(9)+ ϕ(Cγ–Oδ–Cε)(7)
Pair of modes that cross							
59	0.15	0.10	59	τ(Cη–Cη)(32) + τ(Cε–Cη)(29)+ τ(Cβ–Cγ)(13) + τ(Cγ–Oδ)(10)	0.20	59	τ(Cη–Cη)(31) + τ(Cε–Cη)(27)+ τ(Cβ–Cγ)(13) + τ(Cγ–Oδ)(8)
44	0.15	0.10	51	τ(Cα–C)(15) + ϕ(Cη–Cε–Oδ)(15)+ τ(Cε–Oδ)(9) + τ(Cγ–Oδ)(8) + τ(N=C)(7)	0.20	63	τ(Cα–C)(19) + ϕ(Cη–Cε–Oδ)(12)+ τ(Cε–Oδ)(8) + τ(N–Cα)(7)+ ϕ(Cα–Cβ–Cγ)(6)

[a] δ corresponds to repulsion/crossing points.
[b] δ corresponds to the points before/after repels.

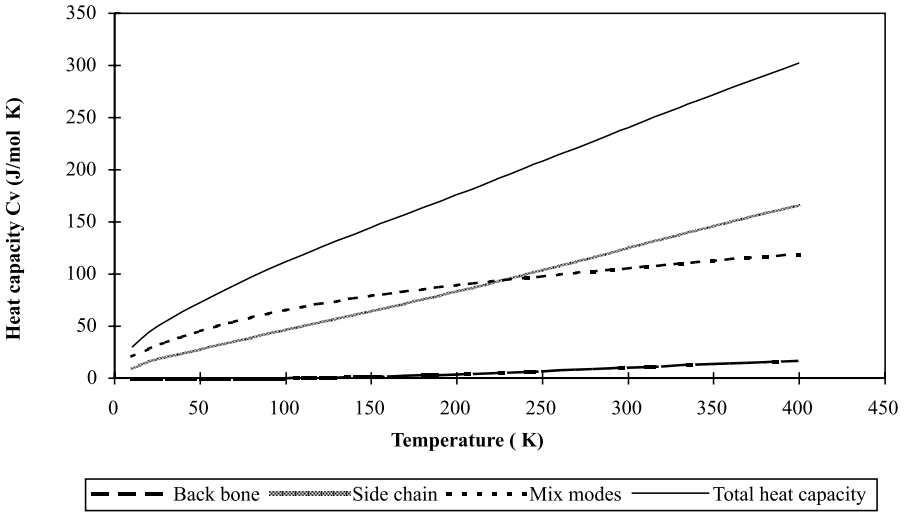

Fig. 6. Variation of heat capacity C_v with temperature for PBLA.

The dispersive behaviour of amide III mode shows completely reverse trend for the two conformations of PBLA. In case of β-PBLA as δ progresses, the energy of the mode decreases whereas for α-PBLA the opposite happens.

The $C\beta H_2$ rocking mode is calculated at 982 cm^{-1} corresponding to the observed peak at 975 cm^{-1}. In case of β-PBLA this mode shows little dispersion ($\sim$12 cm^{-1}) (downward trend), whereas in α-PBLA it shows larger dispersion ($\sim$40 cm^{-1}) (upward trend).

The other interesting features in the dispersion curves include crossing over and repulsion of various branches. All such points correspond to some internal symmetry point in the energy–momentum space and are useful in the interpretation of the spectra and interactions involved. Modes showing crossings, exchange of character and repulsion are listed in Table 9 along with the PED and the δ values at which these features occur. Repulsion between the dispersion curves corresponding to 1110 cm^{-1} (N–Cα stretch) and 1068 cm^{-1} (ring mode) ($\delta = 0$) is observed at $\delta = 0.70\pi$. A pair of mode (mainly bending of ring) at 629 cm^{-1} and a mix mode with ϕ (O⋯C⋯N) and backbone contribution at 597 cm^{-1} approach and repel around $\delta = 0.60\pi$. Another repulsion around $\delta = 0.50\pi$ is seen for a pair of modes calculated at 571 and 538 cm^{-1} at the zone centre.

Crossing is possible for the modes belonging to different symmetry species. Such crossings are possible only for chains having a mirror plane symmetry as in the case of β chain conformation. Crossing occurs for 59 and 44 cm^{-1} pair of modes at $\delta = 0.15\pi$. Here the mode at 59 cm^{-1} is nondispersive whereas the other at 44 cm^{-1} disperses. The lower-frequency modes are generally more sensitive to chain conformation and exhibit greater dispersion.

3.4. Heat capacity

Heat capacity has been calculated as a function of temperature using frequency distribution curves obtained from dispersion curves. The calculated frequency distribution as a function of frequency is shown in Figs. 2(b)–5(b). The predictive values of the heat capacity are shown in Fig. 6. The contributions of pure backbone, pure side-chain and mixed modes to the heat capacity have also been calculated. In β-PBLA there is a greater coupling between motion of side-chain and backbone atoms in comparison to the α form [7]. Hence the contribution of mixed modes to the heat capacity is larger in the β form. It is observed from the figure that the heat capacity contribution of the mixed mode tends to saturate at higher temperature whereas the same for the side chain linearly increases with temperature. The predictive heat capacity values have been reported in the temperature range 10–400 K. It may be mentioned here that at low temperatures (below 100 K) the contribution of the lattice modes is important and would be reflected in the heat capacity. The calculations, taking lattice modes into account would involve solving the problem for the contents of a unit cell instead of a single chain. This will enormously increase the dimension of the matrices to be solved and make the problem extremely difficult both in terms of computer time and in visualising the involved interactions. In spite of these limitations, this work does provide a starting point for further basic studies on the thermodynamical behaviour of polypeptides.

References

[1] Kyotani H, Kanestsuna H. J Polym Sci 1977;15:1029.
[2] Bradbury EM, Carpenter BG, Stephens RM. Biopolymers 1968;6:905.
[3] Kodama H, Tsujita Y, Takizawa A. J Macromol Sci Phys B 1980;17(1):57.
[4] Bradbury EM, Downie AR, Elliott A, Hanby WE. Proc Roy Soc A 1960;259:110.
[5] Karlson RH, Norland KS, Fasman GD, Blout ER. J Am Chem Soc 1960;82:2268.
[6] Goodman M, Felix AM, Deber CM, Brause AR, Schwartz G. Biopolymers 1963;1:371.
[7] Tandon P, Gupta VD, Prasad O, Rastogi S, Katti SB. J Polym Sci Phys 1996;34:1213.
[8] Obata H, Kanetsuna H. J Polym Sci 1971;9:1977.
[9] Kyotani H, Kanetsuna H. J Polym Sci 1972;10:1931.
[10] Alegre C, Guerra SM, Subiana JA. Macromolecules 1989;22:3802.
[11] Gupta VD, Trevino S, Boutin H. J Chem Phys 1968; 48(7):3008.
[12] Krishnan MV, Gupta VD. J Pure Appl Phys 1971;9:1977.
[13] Gupta A, Tandon P, Gupta VD, Rastogi S. Polymer 1997;38:2389.
[14] Burman L, Tandon P, Gupta VD, Rastogi S, Srivastava S. Biopolymers 1996;38:53.
[15] Gupta RS. PhD Thesis, Lucknow University, 1998.
[16] Frushour BG, Koenig JL. Biopolymers 1975;14: 2115.
[17] Wilson EB, Deuis JC, Cross PC. Molecular vibrations: the theory of infrared and Raman vibrational spectra. New York: Dover Publications; 1980.
[18] Higgs PW. Proc R Soc (London) A 1953;220:472.
[19] Benzinger TH. Nature 1971;229:100.
[20] Pan R, Nair VM, Wunderlich B. J Thermal Anal 1989;35:955.
[21] Roles KA, Xenopoulos A, Wunderlich B. Biopolymers 1993;33:753.
[22] Krimm S, Bandekar J. Adv Protein Chem 1986;38:181.
[23] Ambrose EJ, Elliott A. Proc R Soc A 1951;205:47.
[24] Miyazawa T, Blout ER. J Am Chem Soc 1961;83:712.
[25] Srivastava S, Tandon P, Gupta VD, Rastogi S. Polym J 1997;29(6):492.
[26] Krimm S, Abe Y. Proc Natl Acad Sci 1972;69:2788.
[27] Rastogi S, Gupta VD. J Macromol Sci Phys (USA) B 1994;33(2):129.
[28] Burman L, Tandon P, Gupta VD, Rastogi S, Srivastava S, Gupta GP. J Phys Soc Jpn 1995;64(1):308.